© 2017. Published by The Company of Biologists Ltd | Development (2017) 144, 2338-2351 doi:10.1242/dev.143040

Generating minicorneal organoids from human induced pluripotent stem cells

Praveen Joseph Susaimanickam[1,*], Savitri Maddileti[1,*], Vinay Kumar Pulimamidi[1], Sreedhar Rao Boyinpally[2], Ramavat Ravinder Naik[3], Milind N. Naik[4], Geereddy Bhanuprakash Reddy[5], Virender Singh Sangwan[1,6] and Indumathi Mariappan[1,6,‡]

ABSTRACT

Corneal epithelial stem cells residing within the annular limbal crypts regulate adult tissue homeostasis. Autologous limbal grafts and tissue-engineered corneal epithelial cell sheets have been widely used in the treatment of various ocular surface defects. In the case of bilateral limbal defects, pluripotent stem cell (PSC)-derived corneal epithelial cells are now being explored as an alternative to allogeneic limbal grafts. Here, we report an efficient method to generate complex three-dimensional corneal organoids from human PSCs. The eye field primordial clusters that emerged from differentiating PSCs developed into whole eyeball-like, self-organized, three-dimensional, miniature structures consisting of retinal primordia, corneal primordia, a primitive eyelid-like outer covering and ciliary margin zone-like adnexal tissues in a stepwise maturation process within 15 weeks. These minicorneal organoids recapitulate the early developmental events *in vitro* and display similar anatomical features and marker expression profiles to adult corneal tissues. They offer an alternative tissue source for regenerating different layers of the cornea and eliminate the need for complicated cell enrichment procedures.

KEY WORDS: Human induced pluripotent stem cells, Ocular differentiation, Organogenesis, Corneal organoids

INTRODUCTION

Cornea is the transparent, avascular tissue on the ocular surface through which light enters the eye. Any damage to its epithelial, stromal or endothelial cell layers can lead to visual impairment. The annular limbus surrounding the cornea harbors adult stem cells that regenerate different parts of the cornea (Schermer et al., 1986; Cotsarelis et al., 1989). Cell replacement therapy using autologous or allogeneic adult limbal grafts has been the standard treatment for patients with severe limbal stem cell deficiency (LSCD) (Rama et al., 2010; Sangwan et al., 2011; Basu et al., 2016). However, in the case of bilateral epithelial defects and for the treatment of conditions affecting the stromal and endothelial cell layers, alternative stem cell sources such as embryonic stem cells (ESCs) and induced pluripotent stem cells (iPSCs) have been explored with a view to generating the various corneal cell types (Ahmad et al., 2007; Shalom-Feuerstein et al., 2012; Hayashi et al., 2012; Sareen et al., 2014; Mikhailova et al., 2014; Chan et al., 2013; Zhang et al., 2014; Chen et al., 2015; McCabe et al., 2015).

A recent report has shown coordinated development of corneal epithelium, neural crest cells, lens epithelium and retinal cells from iPSCs in a two-dimensional (2D) culture system and employed FACS to establish pure cultures of corneal epithelial cells (Hayashi et al., 2016). However, the requirement of rigorous cell enrichment protocols imposes a major hurdle in tissue-specific cell expansion, but can be overcome by establishing three-dimensional (3D) culture systems. This method exploits the inherent self-organizing capacity of differentiating progenitor cell populations, together with the surrounding niche cells, to generate complex tissue structures *in vitro*. This has been demonstrated successfully with the generation of neuroretinal tissues using PSCs (Eiraku et al., 2011; Gonzalez-Cordero et al., 2013; Assawachananont et al., 2014; Reichman et al., 2014; Zhong et al., 2014; Hiler et al., 2015; Kaewkhaw et al., 2015; Völkner et al., 2016). A recent report has described a method of generating immature corneal organoids from human iPSCs and shown them to express a few corneal markers (Foster et al., 2017). We report here a much simpler and efficient culture method that can generate complex 3D corneal organoids from both human ESCs and iPSCs. We report the establishment of long-term cultures and the characterization of these organoids at different stages of maturation. The mature organoids developed into complex, multilayered, minicornea-like 3D tissues and recapitulated the early developmental events *in vitro*. We also show that they offer an alternative tissue source for various ocular cell types and report the generation of transplantable sheets of corneal epithelium suitable for regenerative applications.

RESULTS

Derivation and characterization of human iPSCs

As pluripotent stem cells are valuable cell sources for generating various ocular cell types and for the study of organ development *in vitro*, we derived and characterized several human iPSC lines from human dermal fibroblasts as described earlier (Takahashi et al., 2007). As shown in Fig. S1A, the hiPSC-F2-3F1 line formed typical ESC-like colonies both on mouse embryonic fibroblast (MEF) feeders and on Matrigel-coated surfaces. This line expanded well under standard human iPSC culture conditions and the cells were passaged more than 25 times. They remained pluripotent and expressed the stem cell markers OCT4 (POU5F1), SOX2, SSEA4 and alkaline phosphatase (Fig. S1B). When passage 25 cells were transplanted into the subcutaneous space of nude mice, they

[1]Sudhakar and Sreekanth Ravi Stem Cell Biology Laboratory, Prof. Brien Holden Eye Research Centre, Hyderabad Eye Research Foundation, L.V. Prasad Eye Institute, Hyderabad 500 034, India. [2]Ophthalmic Pathology Laboratory, L.V. Prasad Eye Institute, Hyderabad 500 034, India. [3]National Centre for Laboratory Animal Sciences, National Institute of Nutrition, Hyderabad 500 007, India. [4]Department of Ophthalmic Plastic and Facial Aesthetic Surgery, L.V. Prasad Eye Institute, Hyderabad 500 034, India. [5]Biochemistry Division, National Institute of Nutrition, Hyderabad 500 007, India. [6]Tej Kohli Cornea Institute, Centre for Ocular Regeneration, L.V. Prasad Eye Institute, Hyderabad 500 034, India.
*These authors contributed equally to this work

‡Author for correspondence (indumathi@lvpei.org)

P.J.S., 0000-0002-1567-1312; V.K., 0000-0002-1365-878X; S.R.B., 0000-0002-2136-4415; R.R.N., 0000-0003-3884-157X; I.M., 0000-0001-7059-3030

Received 30 July 2016; Accepted 19 May 2017

Development (2017) 144, 2338-2351 doi:10.1242/dev.143040

proliferated and developed into teratomas comprising all three germ layers within 6 weeks (n=8, 6/8 animals developed teratomas) (Fig. S1C). The gross karyotype of this female line was found to be normal at passage 20 (Fig. S1D). Genotype analysis confirmed the presence of integrated copies of the three transgenes *OCT4*, *SOX2* and *KLF4*, but not *cMYC*. The endogenous copies of all four genes were active in passage 25 cells and were expressed at levels comparable to that of the human ESC line BJNhem20 (Inamdar et al., 2009; Mariappan et al., 2015) (Fig. S1E).

Eye field differentiation of iPSCs and the development of corneal primordial structures

To induce ocular differentiation, the iPSCs and ESCs were grown to 70-80% confluence under feeder-free conditions and differentiation was initiated *in situ* as described in Fig. 1A. At 4 weeks of differentiation, distinct clusters of raised, circular to oval-shaped eye field primordial (EFP) clusters (or 'EFPs') had developed (Fig. S2A). Starting from 1×10^6 PSCs, an average of 27.33±13.63 EFP clusters could be generated from a well of a 6-well plate (n=6). To confirm that these are EFPs, we manually collected the clusters for total RNA isolation and marker expression analysis by reverse transcription PCR (RT-PCR). As shown in Fig. S2B, the expression of *PAX6*, *OTX2*, *SIX6* and *RX* (*RAX*) confirmed that these 3D clusters consisted of eye field-committed progenitor cells. When the EFPs were allowed to differentiate further *in situ*, they gave rise to lens epithelial clusters (Fig. S2C) and a SEAM (self-formed ectodermal autonomous multizone) of ocular surface epithelium by 6-8 weeks, as described by Hayashi et al. (2016). The central island of neuroretinal (NR) cells was CHX10 $(VSX2)^+$ and $RCVRN^+$, and the SEAM of ocular surface ectodermal (OSE) sheets was P63 $(TP63)^+$ (Fig. 1Bi,ii). A wave of $SOX10^+$ pigmented neural crest cells (NCCs) marked the boundary between NR and OSE cell zones (Fig. 1Biv). Retinal pigmented epithelial (RPE) cells emerged as a compact, non-pigmented epithelium surrounding the NR clusters and later matured to acquire pigmentation. Lentoid clusters expressing gamma-crystallin developed at a precise location adjacent to NR clusters (Fig. 1Bv, Fig. S2C). The NR clusters developed into optic cups and $CHX10^+$ precursors self-organized to form the NR layer (Fig. S2D). Pigmented melanocytes were also observed interspersed within the zone of migrating epithelial cells (Fig. 1Bvi, Fig. S2E).

Apart from the emergence of SEAMs, rare EFP clusters developed into 3D, miniature eyeballs, with transparent anterior-segment-like structures on the surface and complex NR structures beneath. A wave of pigmented NCCs set the boundary for the cornea-like structures (Fig. 2Aiii,iv). When the EFPs at 4 weeks were manually collected and cultured under suspension in non-adherent dishes, 40.05±3.89% gave rise to distinct corneal primordial (CP) structures distinct from the generally observed retinal primordia (RP) (n=6; Fig. 2Avi-ix). In the earlier method described by Hayashi et al. (2016), the corneal epithelial cell enrichment was achieved by approximate zoning of cell outgrowths within the SEAM region and by FACS of $SSEA4^+$ and $ITGB4^+$ cells. However, the method described here enables the self-organization of different CP cells (OSE cells and NCCs) into 3D minicorneal organoids that can directly serve as valuable tissue sources to study corneal development *in vitro* and also to establish pure cultures of different corneal cell types.

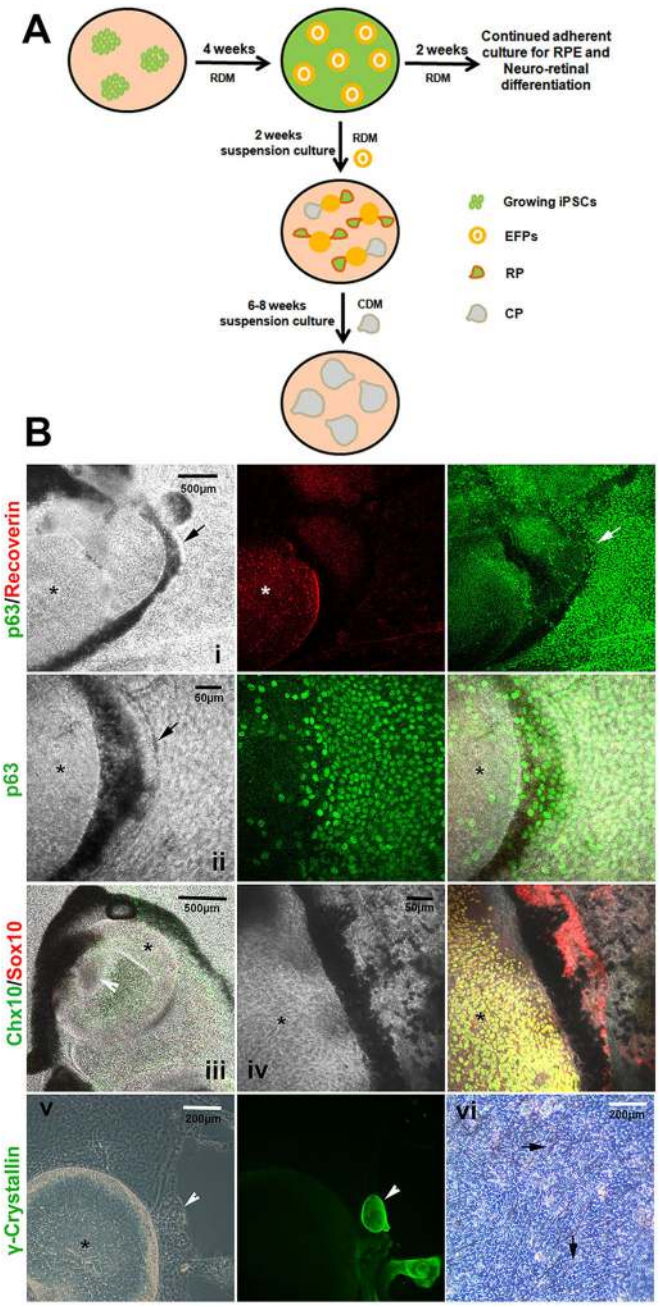

Fig. 1. Characterization of iPSC-derived eye field primordial (EFP) clusters. (A) Schematic representation of the stepwise differentiation of human iPSCs into retinal and corneal organoids. Growing iPSCs are first differentiated into EFPs, which upon isolation and suspension culture give rise to both retinal primordia (RP) and corneal primordia (CP). The dissected-out CP are cultured under corneal differentiation conditions for further maturation. CDM, corneal differentiation medium; RDM, retinal differentiation medium; RPE, retinal pigmented epithelium. (B) Distinct circular to oval-shaped EFPs encompassed a centrally located $CHX10^+$ $RCVRN^+$ neuroretinal (NR) cup (asterisks) (i). Pigmented neural crest-derived cells and $P63^+$ ocular surface ectodermal (OSE) cells appear to differentiate from the edges of EFP clusters. Arrows point to a distinct margin comprising a spindle-shaped melanocyte enriched-zone between the NR and OSE cells (i-iv). Arrowheads point to $crystallin^+$ lentoid clusters adjacent to NR cups (v) and a phase image showing the presence of pigmented melanocytes (arrows) over a layer of epithelial sheet within the migratory cell zone (vi).

Morphological features of minicorneas

The minicorneas (MCs) ranged from ~1-7 mm in diameter (Table S3). A magnified view of MCs revealed the presence of a uniform epithelial cell lining (Fig. 2Aix, Movie 1). Transmission electron microscopy images of an 8-week-old MC revealed the presence of a layer of epithelium with tight junctions and numerous

Development (2017) 144, 2338-2351 doi:10.1242/dev.143040

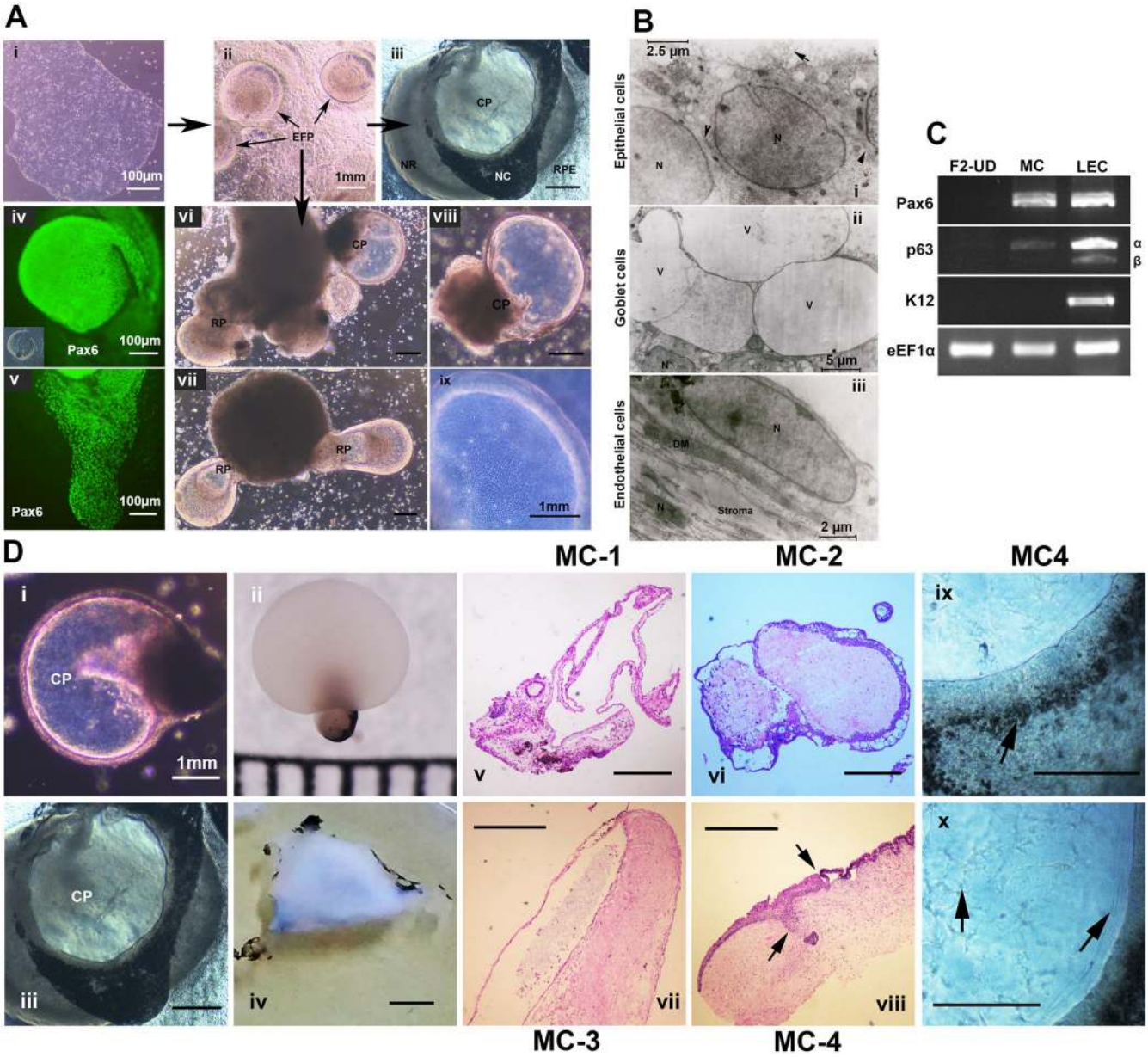

Fig. 2. Morphology of developing corneal organoids. (A) Growing iPSCs (i) differentiate into EFP clusters (ii), which further mature to form whole eyeball-like structures, with transparent CP on the surface and NR cup on the basal side. Pigmented neural crest (NC) cells mark the corneal boundary (iii). Pigmented RPE-like cells are seen migrating out of the NR tissue on the basal side. A subset of PAX6^{+} NR clusters was able to self-organize into optic vesicle-like structure with an optic stalk (iv, inset) and migrating OSE cells (v). Suspension cultures of EFPs gave rise to RP and CP structures (vi,vii), which were isolated and cultured separately for further maturation (viii,ix). *n*=6. (B) TEM images of an 8-week-old minicornea (MC) showing epithelial microvilli (arrow) and tight junctions between cells (arrowheads), cell nuclei (N), microvesicles (v) and Descemet's-like membrane (DM). (C) RT-PCR profiles of 8-week-old MCs, as compared with undifferentiated iPSCs (F2-UD) and primary limbal epithelial cultures (LEC). (D) Representative images of MCs at different stages of development under suspension culture (i,ii) and adherent culture (iii,iv). H&E-stained sections of MCs analyzed (v-viii), showing limbus-like margin (arrows). Magnified view of adherent MC, with pigmented melanocytes (arrows) observed around the corneal periphery and spindle-shaped stromal cell infiltration seen within the transparent CP (ix,x). Scale bars: 1 mm, unless otherwise specified.

apical microvilli, which is a feature of corneal epithelium but not that of lens epithelial cells. The mucin-secreting goblet cells had numerous microvesicles on the apical surface. The middle stromal layer consisted of well-organized collagen fibrils interspersed with stromal cells. A monolayer of flat endothelium-like cells was observed on the inner surface, with a Descemet's-like basement membrane (Fig. 2B). About 10-15 MCs at 8 weeks of differentiation were pooled for the isolation of total RNA, and RT-PCR analysis revealed the expression of the cornea-specific markers *PAX6* and *P63*, but not *K12* (*KRT12*). Variant-specific PCR indicated *P63*α as the major variant expressed in the developing corneas (Fig. 2C).

Maturation of MCs *in vitro*

Hematoxylin and Eosin (H&E) staining of immunohistochemical (IHC) sections of MCs at 6, 8, 10 and 15 weeks of maturation revealed a stepwise process of tissue layer development and self-organization of cells. The transparent MCs grew from 1 to 4 mm in diameter until 10 weeks of differentiation and developed into

Development (2017) 144, 2338-2351 doi:10.1242/dev.143040

opaque structures (Fig. 2Di-iv). The 6-week-old transparent MCs under suspension culture (MC-1) consisted of a double-layered epithelium and a fluid-filled lumen, without any stroma. These structures collapsed immediately after fixation, with leakage of internal fluids (Fig. 2Dv). At ∼8-10 weeks of differentiation, the MCs became strengthened by the subepithelial infiltration of spindle-shaped cells (MC-2), resulting in the development of a thick stromal cell layer, which occupied the entire fluid-filled lumen (Fig. 2Dvi). Surprisingly, IHC examination of intact MCs developing *in situ* in adherent cultures revealed complex tissue patterns, with orderly layers of different cell types that constitute a normal cornea. The adherent MCs at 10 weeks of differentiation (MC-3) revealed the formation of anterior-segment-like structure, consisting of a thin lid-like structure above a cornea-like tissue (Fig. 2Dvii). At 15 weeks of differentiation the adherent MCs exhibited mature corneal features (MC-4), with well-formed corneal and conjunctiva-like surface epithelia, separated by a limbal crypt-like margin zone (Fig. 2Dviii). Pigmented NCCs marked the boundary between the clear corneal surface and the surrounding epithelium (Fig. 2Dix).

Cornea-specific marker expression patterns in floating corneal organoids

To confirm that the MCs are authentic ocular structures and to understand the spatiotemporal distribution of cells within complex tissues, we carried out IHC examinations on MCs at different stages of development (n=8). At 6 weeks, the fragile MC1-1 comprises a double-layered epithelium, with a fluid-filled lumen (Fig. 3Ai). The epithelial cells were VIM^+ $PAX6^-$ $P63^-$, suggesting an undifferentiated primitive state (data not shown). Interestingly, a pair of circular niche-like organizers was observed at the connecting base, and $Ki67^+$ proliferating cells emerged from there (Fig. 3Aii). At 8 weeks, the MC1-2 showed significant stromal cell expansion and stratification of surface epithelium. The basal epithelial cells expressed P63α and PAX6 (Fig. 3Bi,ii) and the entire stroma was populated by VIM^+ cells (Fig. 3Biii). At 10 weeks, the MC-2 developed a thick stratified epithelium, with highly ordered collagen-filled stroma. The epithelial cells expressed P63α, PAX6 and the cornea-specific cytokeratins K3/12 and the stromal cells expressed VIM (Fig. 3C).

Characterization of MCs developing *in situ* on adherent EFPs

At 10 weeks, the MC-3 that developed *in situ* was strikingly similar to a developing anterior segment, with lid-like structures connected by a periderm-like epithelial lining above the corneal surface, as described elsewhere (Findlater et al., 1993; Huang et al., 2009) (Fig. 4A). The stratified corneal surface epithelium expressed PAX6, P63α and low levels of K12; the stromal cells were VIM^+ and the endothelium-like cell layer was VIM^+, $CD200^+$ and $GPC4^+$ (Fig. 4B, Fig. S3A). Infiltrating αSMA^+ cells were observed within the anterior stroma (Fig. 4Biv) and the surrounding adnexal cell layers, possibly indicating the development of smooth muscle structures of limbal vasculatures and Schlemm's canal (Fig. S3B). The stromal, endothelial and lid surface epithelial cells were VIM^+, whereas the stratified corneal epithelial cells were VIM^- (Fig. 4Ci,ii). Interestingly, a pars plicata-like ciliary process with a pigmented epithelium was observed at the periphery of MC-3, as reported previously (Kuwahara et al., 2015; Kinoshita et al., 2016). VIM^+ cell clusters flanked the ciliary processes, suggesting the development of trabecular meshwork and choroid-like structures (Fig. 4Ciii,iv).

The 15-week-old MC-4 was morphologically identical to an adult ocular surface (Fig. 4D), with a distinct limbus-like transition zone separating the $PAX6^+$ $P63\alpha^+$ $K3/12^+$ $K10^-$ corneal epithelium on one side and the periodic acid-Schiff $(PAS)^+$ and Alcian $Blue^+$ goblet cell-enriched epithelium on the other (Fig. 4E, Fig. S3C). The cornea-like structure measured ∼2 mm in diameter (∼1/6th the size of an adult cornea) and expressed most of the cornea-specific markers observed in adult corneal tissues (Fig. S4). The goblet cells were $PAX6^-$ $P63^-$, which suggested their development from OSE independent of *PAX6* and *P63* regulation. Surprisingly, except for a few newly emerging cells, the majority of the goblet cells did not express the adult conjunctival goblet cell-specific mucin MUC5AC (Fig. 4Evi). Therefore, we further checked for expression of the other secretory mucin, MUC2. IHC examinations confirmed that the goblet cells were $MUC2^+$ (Fig. 4Ev). Interspersed between the goblet cells were a few brightly stained $PAX6^+$ and $K19^+$ epithelial cells (Fig. 4Ei, Fig. S5Bvii), which suggests the late emergence of conjunctival epithelium and its dependence on *PAX6* for development and maturation. Interestingly, a distinct vasculature-like structure with a central lumen and αSMA^+ cell lining was observed within the stroma of the transition zone. CD34 staining indicated the presence of vascular endothelium-like cells on the inner lining of the lumen, thus confirming the initiation of vascular network development along the conjunctival margin (Fig. S5Avii,viii). Another cluster of spindle-shaped $CD34^+$ cells in the peripheral stroma indicated the emergence of a mesenchymal cell wave (Fig. S5Bix).

A periderm lining in developing MC structures

The frequent detachment of an intact epithelial monolayer from the MC surface suggested that it constitutes a separate cell layer that is possibly embryonic periderm in origin. Mouse skin periderm cells are known to emerge from $P63^+$ surface epithelium during the early stratification events and are $P63^-$, $K17^+$ and $K6^+$ (Richardson et al., 2014). During development, the periderm layer plays an important role in preventing pathological cell adhesions between the epithelial linings of adjacent organs, thus ensuring normal tissue formation. Our IHC examinations confirmed that the limbal stem cell marker K15 was exclusively expressed by the basal epithelial cells and that K13 marked the surface and suprabasal epithelium, as reported previously (Ramirez-Miranda et al., 2011; Yoshida et al., 2006). Also, the entire epithelium of MC-2, including the loose surface layers, expressed K13 and the periderm markers K17 and K19 (Fig. 5A). In MC-3, the corneal surface, lid surface and the connecting periderm were lined by $K17^+$ and $K19^+$ cells (Fig. 5B). When we examined the adult tissues, we observed that the flat wing cells at the corneal epithelial surface retained K13 and K19 expression, while the entire adult ocular surface epithelium was $K17^-$ (Fig. S6).

Lid and corneal surface epithelial margins in developing organoids

The lid, forniceal and bulbar conjunctiva, limbal and corneal surfaces are lined by a contiguous sheet of epithelium and are distinguished based on minor differences in marker expression and the presence of additional cell types, such as the conjunctival goblet cells. It is well known that the basal cells of the entire epithelial lining express P63 (Fig. S7i). However, the eye-specific PAX6 is expressed only by the corneal and conjunctival epithelial cells (Fig. S7ii). To check if such higher-order cellular organization becomes established in mature corneal organoids, we examined 15-week-old MCs (MC-5) in long-term suspension cultures. As the organoids matured, the lid structures expanded simultaneously and occupied the major volume. The basally positioned corneal structure showed a remarkable cellular organization, with surface epithelium and orderly arranged, compact stromal cells, resembling

Development (2017) 144, 2338-2351 doi:10.1242/dev.143040

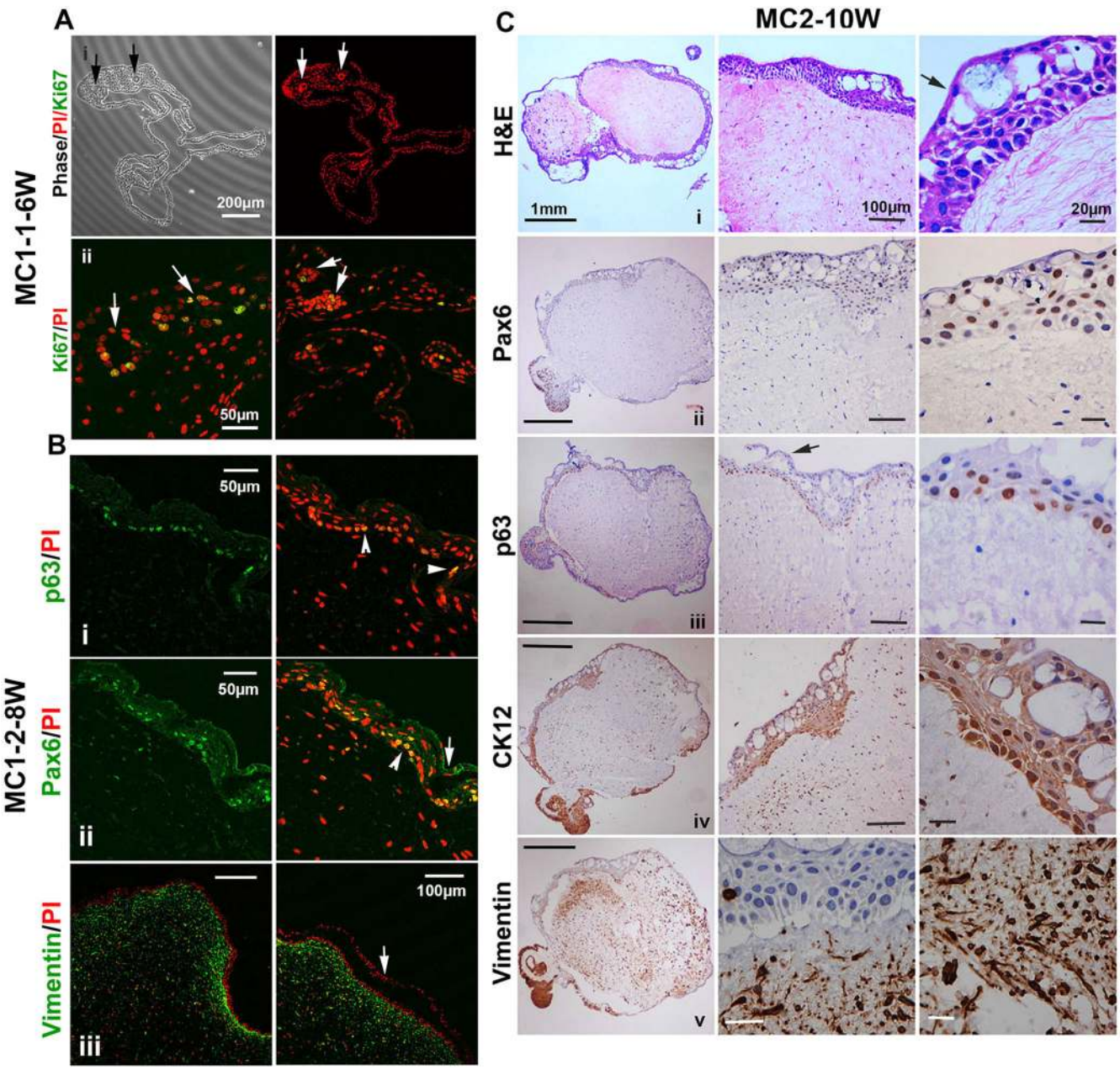

Fig. 3. IHC characterization of 6- to 10-week-old floating organoids. (A) IHC sections of 6-week-old MC1-1 showing a niche-like organizer region populated by Ki67$^+$ cells (i,ii). (B) IHC sections of 8-week-old MC1-2, immunostained for P63 (i), PAX6 (ii) and VIM (iii) (green) and counterstained with PI (red). Arrowheads point to P63$^+$ and PAX6$^+$ basal epithelium. Arrows indicate the loosely detaching surface epithelium. (C) Brightfield images of tissue sections of 10-week-old MC2 stained with H&E (i) or immunostained for PAX6 (ii), P63 (iii), K12 (iv) or VIM (v). DAB-stained sections (brown) were counterstained with Hematoxylin (blue).

that of a mature corneal tissue. Similar to MC1-1, a niche-like organizer formed the origin of P63$^+$ cells, which appeared to be migrating away from the center in an outward spiraling fashion, as a double-layered epithelium (Fig. 6i). The lid epithelium was stratified and the basal cells expressed P63. However, PAX6 expression was limited to the corneal surface epithelium, with very weak or no expression in epithelial cells along the lid margins (Fig. 6iii). Similarly, K10 expression was restricted to the lid surface epithelium, with negligible expression in the corneal epithelium (Fig. 6iv). The corneal epithelial basal cells were PAX6$^+$ P63$^+$, whereas the mature suprabasal cells were PAX6$^+$ P63$^-$ (Fig. 6v). Other adnexal structures, such as the lentoid bodies derived from OSE, could be identified as PAX6^{high} αA-crystallin$^+$ P63$^-$ cell clusters (Fig. 6ii,iii). In addition to the lens, the surface epithelial cells also expressed αA-crystallin, as observed in developing mouse eyes (Fig. S7iii).

Limbal margin establishment and delayed emergence of conjunctival epithelium

In 15-week-old adherent MC-4, P63$^+$ basal cells were restricted to the corneal side and MUC2$^+$ goblet cells were restricted to the conjunctival side, at the transition zone (Fig. 4Eii). In agreement with an earlier report (Richardson et al., 2014), upon epithelial stratification K17 expression became downregulated in the surface periderm cells, and the basal epithelial stem cells were P63$^+$ and K17$^+$ (Fig. 7Ai) and established a clear transition zone resembling that of a limbal margin. The abundance of Ki67$^+$ proliferating cells within the goblet cell-enriched epithelium indicates that the

Development (2017) 144, 2338-2351 doi:10.1242/dev.143040

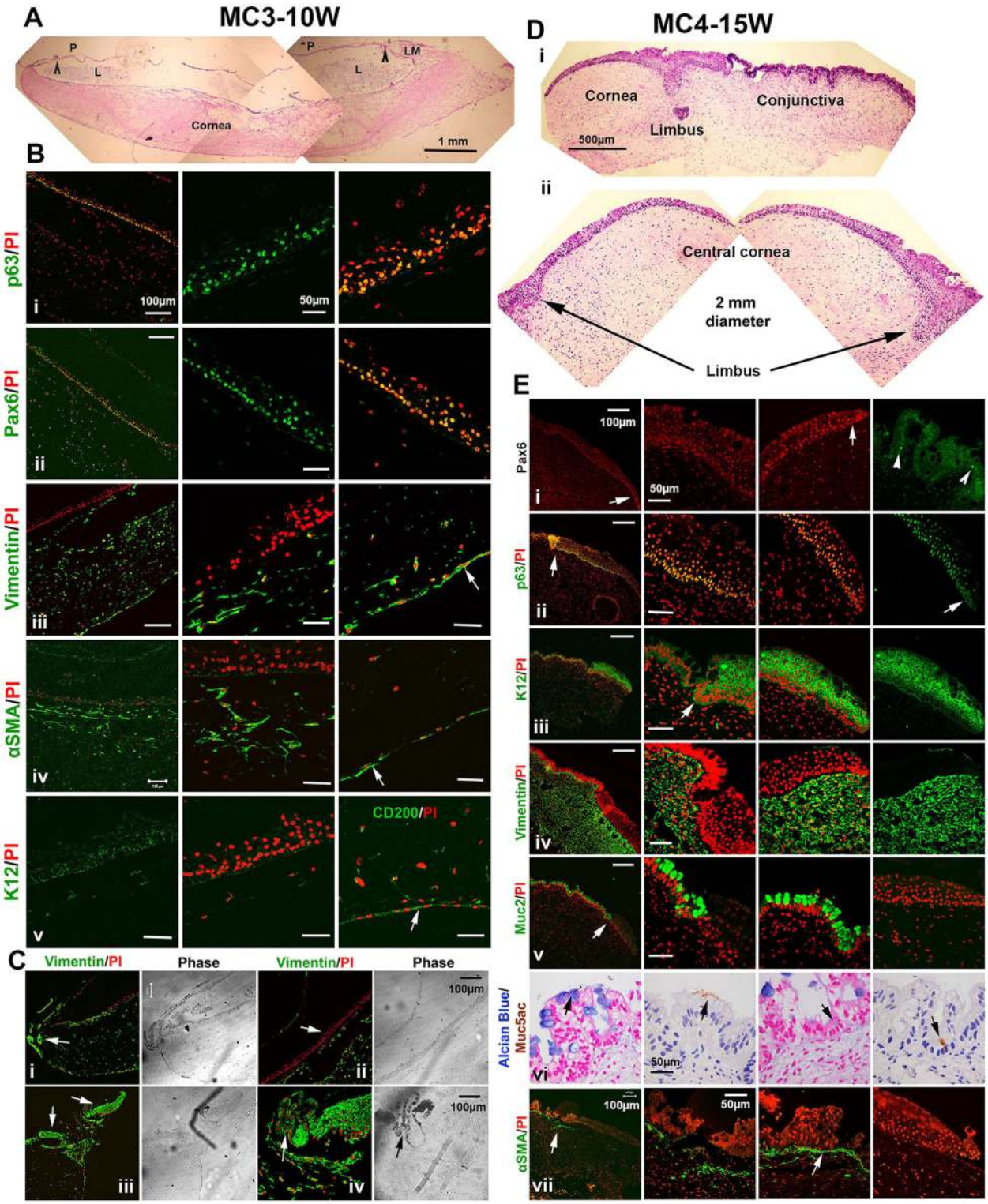

Fig. 4. IHC characterization of 10- to 15-week-old adherent MCs. (A) H&E-stained sections of 10-week-old MC3 shows a thick stroma lined by a thin monolayer of epithelium-like and endothelium-like cells on either side and a lid margin (LM) on the top (arrowhead), connected by a thin periderm-like (P) continuous epithelial lining covering the entire ocular surface, with a fluid-filled lumen (L) in between. (B) Confocal images of tissue sections of MC3, immunostained for P63 (i), PAX6 (ii), VIM (iii), αSMA (iv), K12 and CD200 (v) (green) and counterstained with PI (red). Arrows point to the endothelial cell layer. (C) The corneal surface epithelium (arrow) of MC3 is a VIM^{-} (ii), ciliary margin-like structure formed by ruffled pigmented epithelial cells (iv) and flanked by VIM^{+} ocular adnexal structures (iii). (D) H&E-stained sections of 15-week-old MC4 reveal mature cornea-like features, such as a thick stromal layer lined by a stratified squamous epithelium on the apical surface. A limbus-like structure separates the cornea-like epithelium and the goblet cell-enriched future conjunctiva. (E) Confocal images of tissue sections of MC4 immunostained with PAX6 antibody in red (i), or stained for P63 (ii), K12 (iii), VIM (iv), MUC2 (v) or αSMA (vii) in green and counterstained with PI in red. Brightfield IHC images are shown of sections stained with MUC5AC antibody (arrows) and Alcian Blue and counterstained with Hematoxylin or Nuclear Fast Red, respectively (vi).

Development (2017) 144, 2338-2351 doi:10.1242/dev.143040

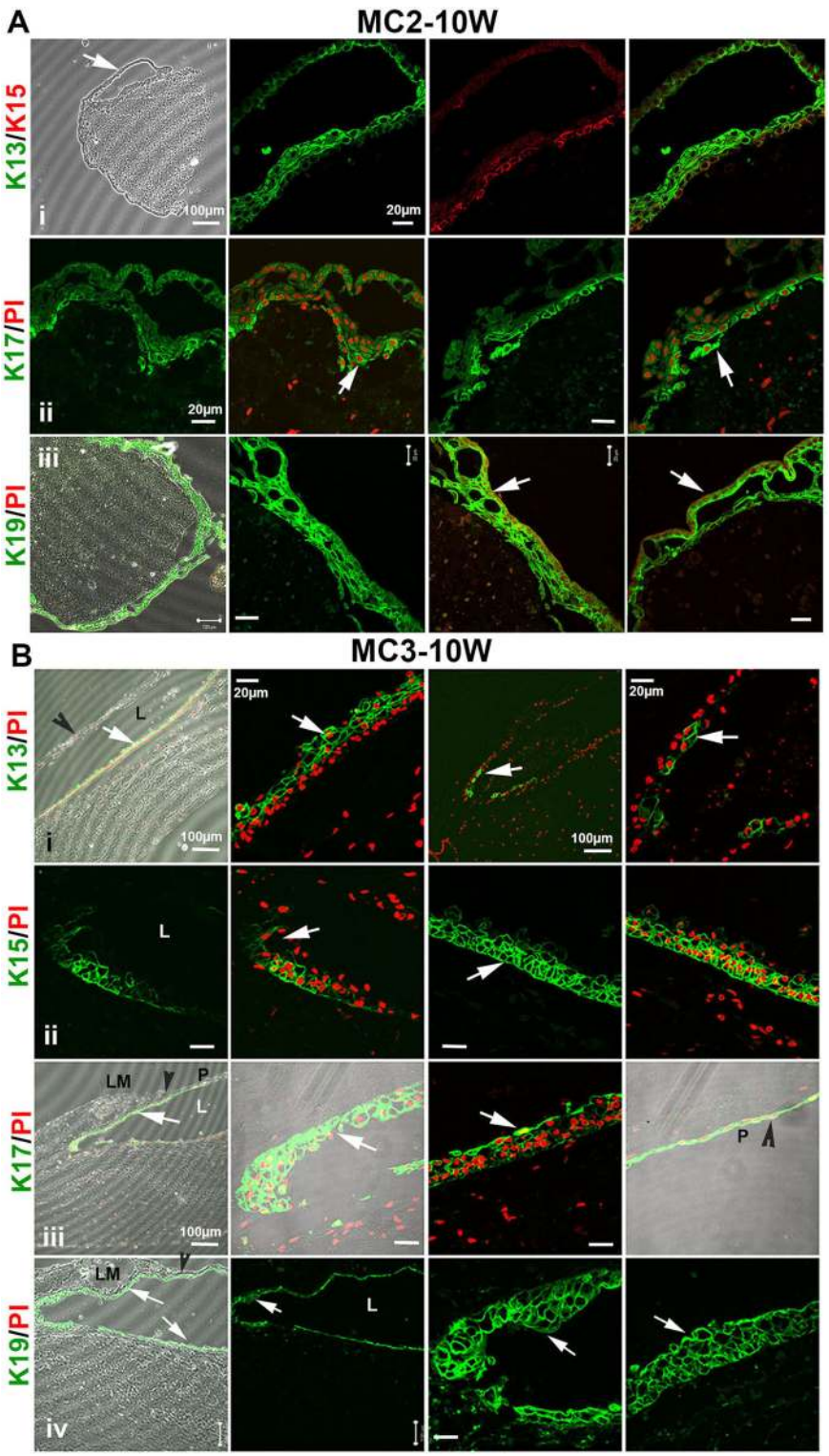

Fig. 5. Expression of periderm markers in floating and adherent MCs. (A) Confocal images of immunostained tissue sections of MC2 showing the expression of different keratins in green. The basal cells were $K15^+$, while the suprabasal cells and the apical lining were $K13^+$ (i). The basal cells also expressed K17 (arrows) (ii). However, the entire stratified epithelium and the loosely adhered, periderm-like flat surface lining cells (arrows) expressed K19 (iii). The sections were counterstained with PI to mark the nuclei in red. (B) The expression of cytokeratin markers shows a clear demarcation within the developing epithelium of a 10-week-old MC. The surface and suprabasal epithelium on the corneal surface express K13 and the expression disappears at the lid margin in the forniceal epithelium (i). K15 expression was observed in basal corneal epithelial cells and was absent at the corneal and lid surface junction (ii). The periderm, lid margin and the apical flat cell layer of the corneal epithelium showed intense K17 staining (iii). The entire epithelial lining of the developing ocular surface expressed K19 (iv). Lid margins (LM) are marked by arrowheads. The lid periderm (P) was observed as a thin continuous sheet of epithelium covering the entire corneal surface, with a fluid-filled lumen (L) in between.

progenitor cell proliferation, differentiation and tissue expansion proceed from the transition zone (Fig. 7Aii). Dual staining for MUC2 and P63 or K3/12 expression further confirmed the presence of a transition zone (Fig. 7Aiii,iv). The surface epithelium formed a collagen IV-enriched basement membrane, while the VIM^+ stromal cells laid out a well-organized collagen I-enriched extracellular matrix (Fig. 7Av,vi). When the expression patterns of other epithelial keratins were examined, we observed that $K13^+$, $K15^+$ and $K17^+$ cells were restricted to the limbal margin. Within the stratified corneal epithelium, K13 marked the surface and suprabasal cells, while K15 and K17 marked the basal and suprabasal cells (Fig. 7B). However, all of the surface epithelial cells expressed K19, with intense staining in the basal cells, surface periderm-like cells and in a few developing conjunctival epithelial cells, which suggested the late emergence of conjunctival epithelium.

Development (2017) 144, 2338-2351 doi:10.1242/dev.143040

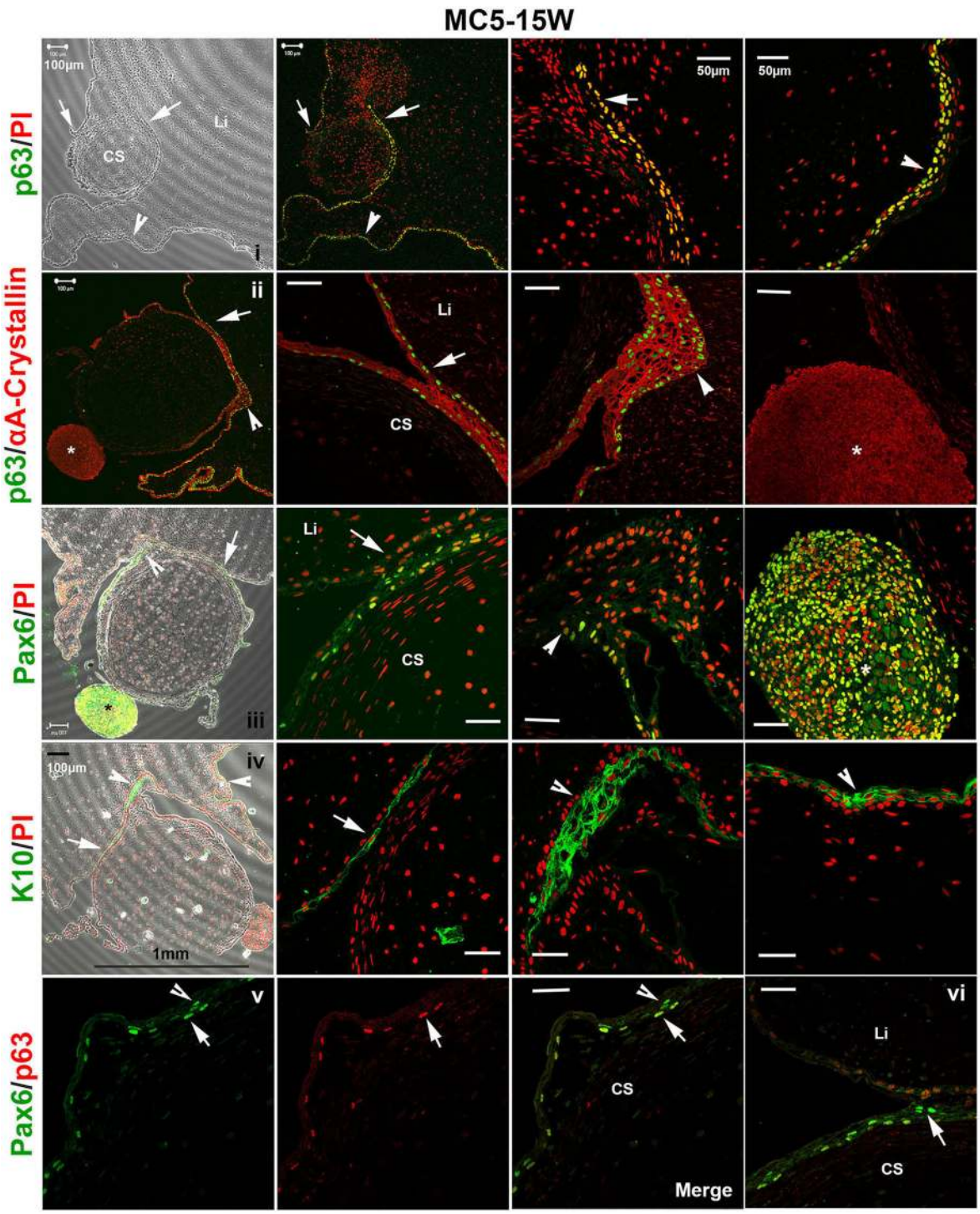

Fig. 6. IHC characterization of 15-week-old mature corneal organoid in suspension. Confocal images of tissue sections of MC5, showing a basally located MC with well-developed corneal stroma (CS) of ∼1 mm diameter. The lid-like tissue (Li) became expanded on the apical surface. The first column of all panels (i-iv) represents a lower magnification view and columns 2-4 are higher magnification views of the regions marked by arrows, arrowheads and asterisks. The $P63^{+}$ epithelial cells seem to arise from a pair of niche-like organizers within the corneal stroma and formed the corneal and lid surface epithelium (i). The basal cells of the entire epithelial lining expressed P63 and co-expressed αA-crystallin. Lentoid clusters (asterisks) are distinguished as $P63^{-}$ αA-crystallin^{+} cells (ii). Pax6 expression is limited to the corneal surface epithelium and the cells within the lentoid clusters. The anterior corneal stroma (CS) is well developed with flattened and compactly arranged stromal keratocytes, as observed in adult corneal tissues (iii). The epithelial lining on the lid surface adjoining the corneal surface showed weak PAX6 nuclear expression and was $K10^{+}$ (iv). The basal cells of the stratified corneal epithelium were $P63^{+}$ $PAX6^{+}$ (arrows), while the differentiated apical cells were $P63^{-}$ $PAX6^{+}$ (arrowhead). Columns 3 and 4 indicate two different merged images (v, vi).

Characterization of cell outgrowths from EFPs

When the cell outgrowths from EFPs were analyzed in adherent 2D cultures, we found that $SSEA4^{+}$ primordial cells tended to organize into ruffled structures resembling limbal crypts and gave rise to $P63^{+}$ and $PAX6^{+}$ ocular surface epithelial cells (Fig. 7Ci-iii, Movies 2 and 3) and waves of NES^{+}, $SOX10^{+}$ and $PAX6^{low}$ NCCs.

Development (2017) 144, 2338-2351 doi:10.1242/dev.143040

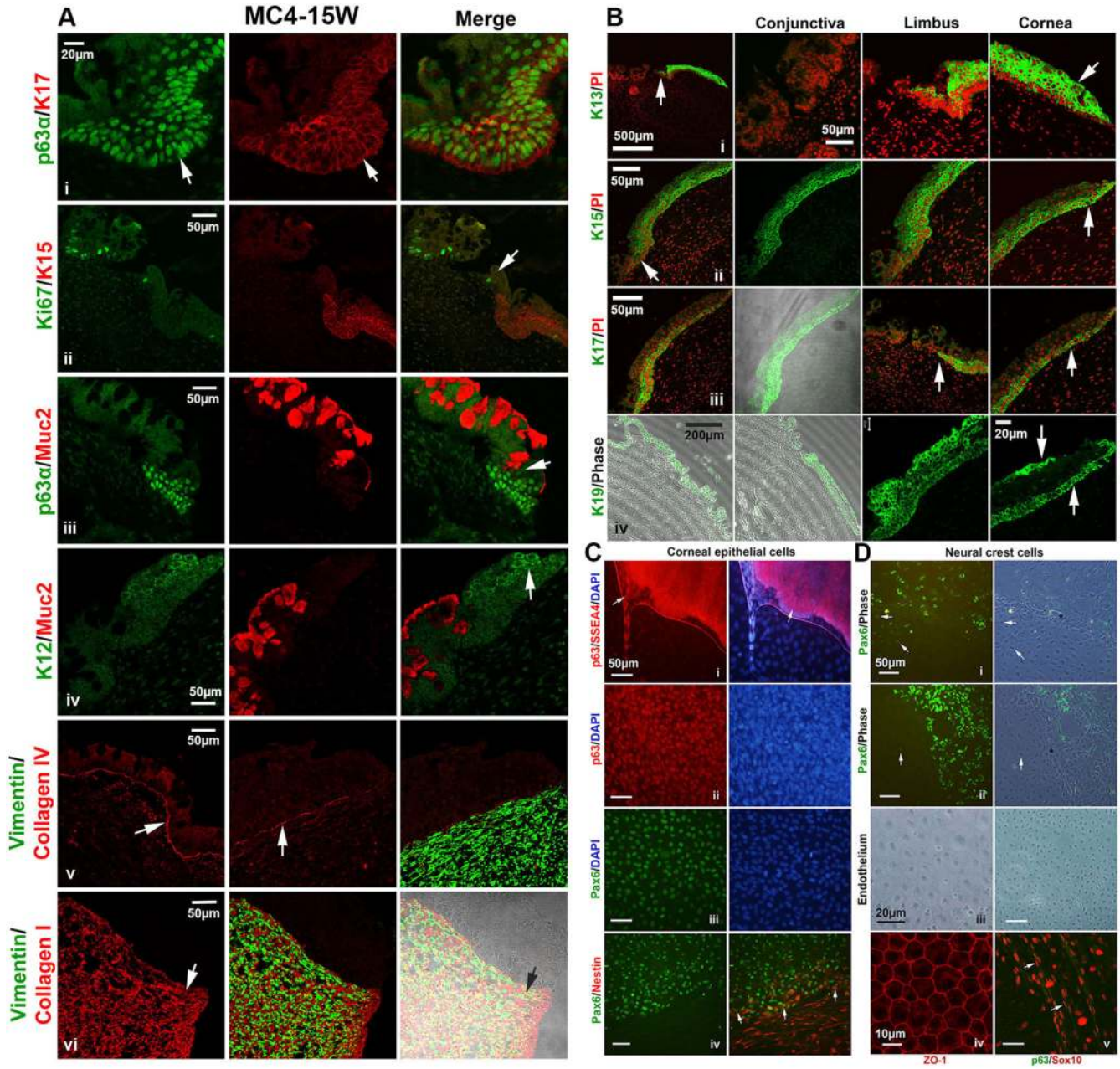

Fig. 7. Mature cornea-specific marker expression in MCs and cell outgrowths from tissue explants. (A) Confocal images of tissue sections of MC4 co-immunostained for P63α and K17 (i), KI67 and K15 (ii), P63α and MUC2 (iii), K12 and MUC2 (iv), VIM and COL4A1 (v), VIM and COL1A1 (vi). Arrows mark the limbus-like margins (i-iii), $K12^+$ corneal epithelium (iv), basement membrane (v) and the stromal matrix (vi). (B) Confocal images of tissue sections of MC4 immunostained for K13 (i), K15 (ii), K17 (iii) and K19 (iv). Note the surface epithelial expression patterns of K13 and K19, while K15 and K17 mark the basal epithelial stem cells. Apart from weak K19 expression, the conjunctival epithelium was negative for all the keratins tested. The limbus-like margins are indicated by arrows in the first column. $K13^+$ suprabasal cells (i), and $K15^+$ (ii), $K17^+$ (iii) and $K19^+$ (iv) basal cells of central corneal epithelium are indicated by arrows in the last column. (C) OSE outgrowths from EFPs formed a ruffled, limbal crypt-like arrangement of $SSEA4^+$ cells at the proximal end, giving rise to migrating $P63^+$ epithelial stem cells (arrows) (i). The outgrowths from explants result in uniform corneal epithelial sheets containing $P63^+$ (ii) and $PAX6^+$ (iii) cells. $PAX6^+$ epithelial sheets (green) are lined by NES^+ NCCs (red). Arrows indicate the double-positive cells at the boundaries (iv). (D) $PAX6^{low}$ NCC patches downregulate PAX6 expression (arrows) and morphologically differentiate into hexagonal, corneal endothelium-like cells (i,ii), with distinct $ZO\text{-}1^+$ tight junctions between the cells (iii,iv). The migratory NCCs are $SOX10^+$ $P63^-$ (arrows) (iv). DAPI (blue) and PI (red) were used as counterstains. Scale bars: 50 µm, unless otherwise specified.

NES^+ cells are a component of the native limbal niche (Fig. S4x) and we show that iPSC-derived $PAX6^+$ epithelial outgrowths are lined by NES^+ NCCs that co-express PAX6, as reported previously (Mariappan et al., 2014) (Fig. 7Civ). Patches of $PAX6^{low}$ neural crest-like cells differentiated into a corneal endothelium-like phenotype by downregulating PAX6 (Fig. 7Di,ii); they appeared as hexagonal, compactly arranged, non-pigmented flat cells with ZO-1 $(TJP1)^+$ tight junctions (Fig. 7Diii,iv). The migratory NCCs were found to be $SOX10^+$ $P63^-$ cells (Fig. 7Dv).

Characterization of corneal organoid-derived transplantable cell sheets

Explant cultures of 8- to 10-week-old MCs on glass coverslips resulted in a spiraling wave of $P63^-$ $K17^+$ OSE cells at the leading edge,

Development (2017) 144, 2338-2351 doi:10.1242/dev.143040

followed by a compactly arranged monolayer of P63^{+} K17^{+} corneal epithelial cells (Fig. S8). In an attempt to generate transplantable sheets of corneal epithelium, we established explant cultures on denuded human amniotic membrane (hAM) substrates, using mature cornea-like organoids at 8-10 weeks of maturation. IHC examination of 10-day-old cultures confirmed that the uniform sheets of PAX6^{+} K12^{+} epithelium generated using corneal organoids were comparable to those generated using adult limbal explants. The basal epithelial cells were PAX6^{+} P63^{+} P75 (NGFR)$^{+}$ and also expressed K17, K19 and VIM (Fig. 8). Interestingly, the resting corneal epithelium was found to

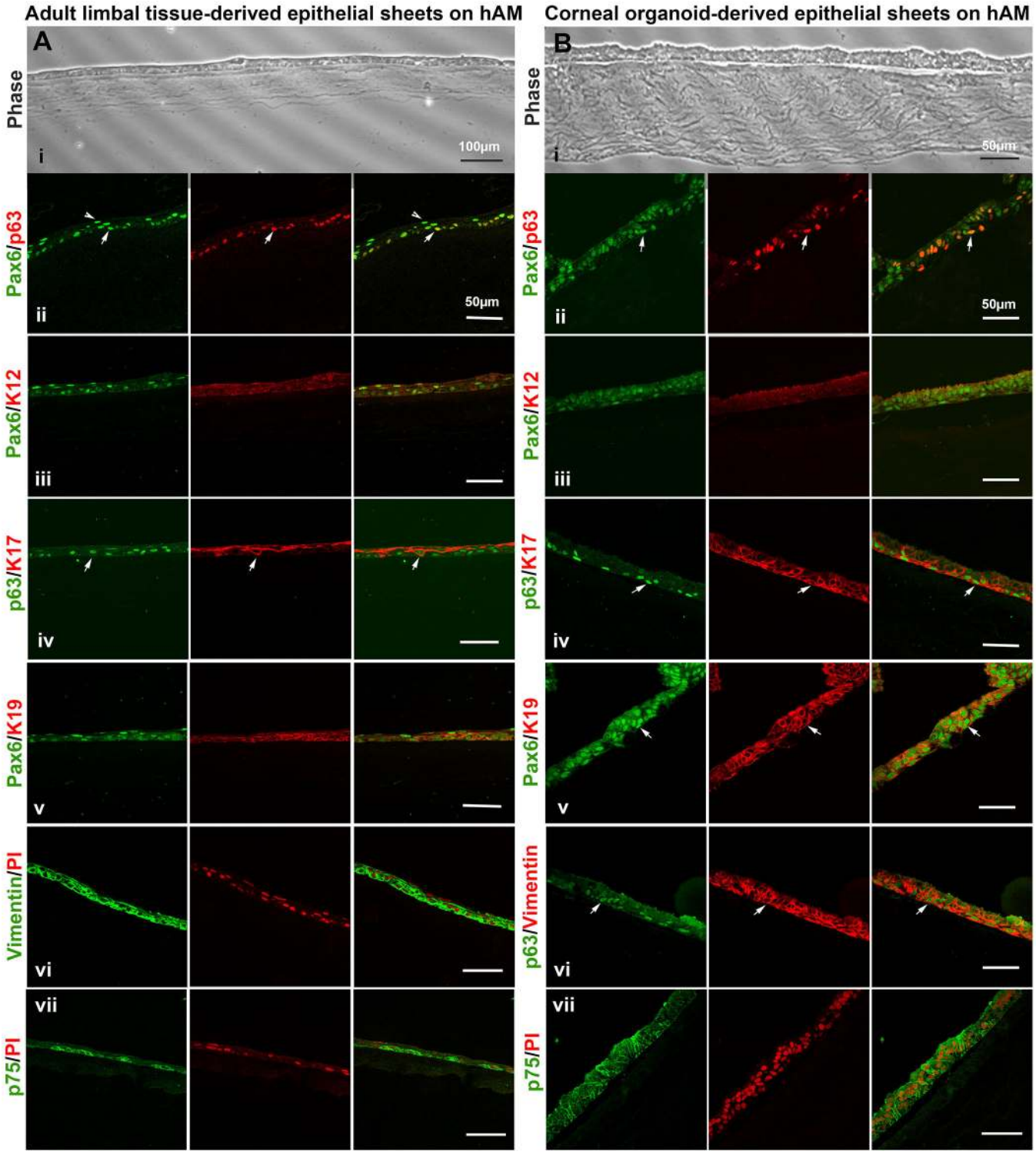

Fig. 8. Organoid-derived transplantable corneal epithelial grafts on human amniotic membrane substrate. (A) Confocal images of tissue sections of epithelial grafts generated using adult limbal tissues and (B) iPSC-derived corneal organoids on denuded hAM (i). Both the engineered grafts were comparable in terms of spatial distribution and expression patterns of corneal epithelium-specific markers such as PAX6, P63, K12 (ii-iii); cytoskeletal proteins such as K17 (iv), K19 (v) and VIM (vi); and of the basal stem cell marker P75 (vii). Arrows indicate the dual positive basal epithelial cells (ii-v). Arrowheads indicate the PAX6^{+}P63^{-} suprabasal cells (ii).

Development (2017) 144, 2338-2351 doi:10.1242/dev.143040

be VIM$^-$ K17$^-$ (Figs 4 and 6). However, the actively proliferating cells in both the limbal and organoid explant cultures were VIM$^+$ K17$^+$, suggesting a possible activation of these markers during acute regeneration and wound healing responses.

DISCUSSION

An autologous iPSC-derived corneal cell source will offer a promising alternative for the treatment of patients with bilateral LSCD. A few earlier reports have demonstrated the possibility of deriving PAX6$^+$ P63$^+$ K3/12$^+$ corneal epithelial cells from PSCs in 2D cultures. Here, we report for the first time an efficient method of generating complex 3D corneal organoids using iPSCs, which circumvents the need for complicated cell enrichment procedures as are involved in establishing limbal cultures.

The adoption of a simple differentiation protocol by the direct shifting of growing cultures to retinal differentiation conditions in the absence of noggin has resulted in successful induction of EFP clusters. We also emphasize that it is crucial to excise EFPs and initiate suspension cultures at 4 weeks of differentiation, before the commencement of surface ectodermal cell and NCC migration, in order to ensure successful induction of corneal organoids in ∼40% of the EFPs by 6 weeks. We believe that the inhibition of migration of proliferating progenitor cells away from EFPs in suspension culture enables the autonomous self-assembly of various cell types, resulting in the generation of complex 3D corneal organoids.

The bilayered epithelium of the newly emerged MCs was derived from the primitive periderm-like P63$^-$ PAX6$^-$ VIM$^+$ OSE cells. The presence of internal fluid appears to help in establishing a circular and convex shape for the developing corneas. The subsequent wave of VIM$^+$ stromal cells and the deposition of collagen matrix helped to strengthen the outer scaffold of OSE cells. The developing lid-like structure in MC-3 was lined and connected by a continuous periderm-like epithelium above the corneal surface. This observation is in agreement with the fact that the developing eyelids fuse and form a continuous covering over the developing cornea. The connecting periderm disintegrates and enables lid separation and eye opening during advanced stages of embryonic development in humans and at postnatal stages in rodents (Findlater et al., 1993; Huang et al., 2009). Unlike the developing skin periderm that is shed after birth (Richardson et al., 2014), the presence of K13$^+$ K17$^+$ K19$^+$ periderm-like surface epithelium in developing MCs and in adult corneas suggests their probable role in normal ocular surface development and in adult tissue homeostasis. We hypothesize that this unique surface lining may help in preventing abnormal cell fusions between the corneal and lid surface epithelium during embryonic eye development and in wound repair processes during adult tissue regeneration.

The presence of ciliary margin zone (CMZ)-like pigmented and ruffled epithelium, flanked by VIM$^+$ structures, at the corneal periphery prompted us to speculate that CMZ development might precede or coincide with ocular surface periderm formation (∼5-6 weeks). The secretions of the CMZ cells might contribute to setting the initial corneal shape, which becomes further strengthened by the infiltration of VIM$^+$ NCCs. The NCCs also contributed to the formation of a monolayer of VIM$^+$ CD200$^+$ GPC4$^+$ endothelium-like cells beneath the thick stroma, thus resulting in the generation of a complete anterior-segment-like structure.

As the MCs matured, the lid and the limbal margins became established by the spatiotemporal pattern of expression of P63, PAX6 and keratins. The P63$^+$ cells were restricted to the corneal and limbal basal epithelial cells, thus establishing a sharp boundary between the cornea and the future conjunctiva. Whereas the entire surface epithelium expressed PAX6 at low levels, well-differentiated central corneal cells and a subset of cells within the conjunctival region were brightly PAX6$^+$, confirming its key role in corneal maturation and the emergence of conjunctival epithelium. The majority of the goblet cells on the conjunctival side were MUC2$^+$ P63$^-$ PAX6$^-$, which suggests that the goblet cells emerge from the primitive OSE cells independently of P63 and PAX6 expression. However, the adult conjunctival goblet cells expressed very low levels of MUC2 (McKenzie et al., 2000) and were predominantly MUC5AC$^+$ (Fig. S4Av). An earlier report has confirmed that goblet cell development is normal in *Muc5ac*$^{-/-}$; *Muc5b*$^{-/-}$ mice (Marko et al., 2014). Taken together, we believe that MUC2 and MUC5AC are the developing and mature conjunctival goblet cell markers, respectively. The presence of niche-like organizing structures consisting of Ki67$^+$ P63$^+$ cells suggests that the tissue growth and expansion proceeds from such transition zones. Further anatomical maturation of corneal tissue was mediated by the infiltration of CD34$^+$ mesenchymal stem cells (Sidney et al., 2014) and other neural crest-derived cell types, such as the smooth muscle cells, which contributes to the formation of limbal and episcleral vasculatures.

Earlier evidence has confirmed the roles of *PAX6* in regulating NCC migration and their differentiation into ocular cell types (Baulmann et al., 2002; Kanakubo et al., 2006) and the involvement of NCC-dependent signaling in feedback regulation on *PAX6* (Grocott et al., 2011). Our observations indicate that the PAX6^{low} NCCs differentiated into flat, non-pigmented, endothelium-like hexagonal cells by downregulating PAX6 expression. Explant cultures of 8- to 10-week-old MCs on hAM has enabled the generation of transplantable sheets of PAX6$^+$ P63$^+$ K12$^+$ corneal epithelial sheets, similar to adult limbal tissue-derived grafts intended for regenerative applications. We further plan to use these tissue grafts in xenotransplantation studies in rabbit LSCD models, to test their clinical suitability in corneal surface reconstruction procedures.

Conclusions

In summary, we show for the first time that complex 3D corneal organoids can be generated from iPSCs and that the MCs undergo maturation *in vitro* and recapitulate the steps of normal corneal development, as depicted in Fig. 9. The availability of such MCs at 10 weeks of maturation circumvents the need for complicated cell enrichment protocols and offers a simpler method of establishing enriched cultures of corneal epithelial cell sheets for basic research needs and for regenerative applications.

MATERIALS AND METHODS

Ethics

This study was approved by our Institutional Review Board (IRB) of the LV Prasad Eye Institute, Hyderabad, India. All research involving human samples followed the tenets of the Declaration of Helsinki. Experiments involving animals were conducted in adherence to the ARVO statement for use of animals and with the approval of the Institutional Animal Ethics Committee (AEC) of the National Institute of Nutrition, Hyderabad, India.

Derivation and maintenance of human iPSCs

Full-thickness punch biopsies of skin were taken from volunteers with their informed consent. The biopsies were used to establish human dermal fibroblast (HDFs) cultures. A retroviral cocktail containing individual vectors expressing the *OCT4*, *SOX2*, *KLF4* and *cMYC* (OSKM) transgenes were used to transduce passage 3 HDFs at an MOI of ∼2. The cells were then split and cultured under standard human ESC culture conditions. The reprogrammed clones that emerged after 3 weeks were manually picked

Development (2017) 144, 2338-2351 doi:10.1242/dev.143040

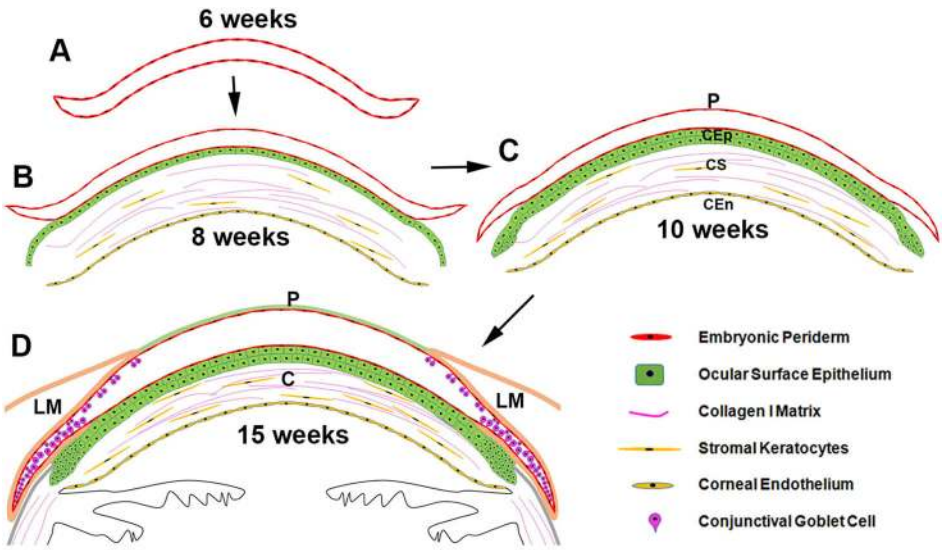

Fig. 9. Illustration of the different stages of MC development *in vitro*. (A) The transparent, bubble-like CP at 6 weeks of development consisted of a double-layered primitive embryonic periderm-like epithelium, with a fluid-filled lumen. (B) NCCs migrate into the subepithelial space at ∼8 weeks to form a thick stroma and an endothelium-like monolayer. This establishes and strengthens the corneal matrix. (C) The ocular surface epithelium (OSE) developed and stratified over the stably established stromal matrix at ∼10 weeks. The OSE remained sandwiched between the stroma and the periderm-like surface lining (P). P63α^{high} and PAX6^{low} cells appeared in the basal cell layers. The periderm lined the entire ocular surface and also formed a continuous outer covering for the developing anterior segment. (D) The lid-like structures developed on either side, connected by an intact periderm. Mature cell markers such as PAX6 and K12 became induced in the stratified OSE at ∼15 weeks. Goblet cells developed within the future conjunctival and forniceal surface epithelium, independently of PAX6 and P63 expression. C, cornea; CEp, corneal epithelium; CEn, corneal endothelium; CS, corneal stroma; LM, lid margin.

based on colony morphology and five clones were passaged for further expansion. The clones were also adapted to feeder-free culture conditions on Matrigel (Corning) coated plates using the mTeSR™1 kit, as per manufacturer's instructions (STEMCELL Technologies). The reprogramming efficiency was 0.005% and the clone hiPSC-F2-3F1 was expanded beyond 25 passages and characterized for stemness and pluripotency.

Eye field differentiation of human iPSCs and ESCs

Growing cultures of the human ESC line BJNhem20 and the normal human iPSC line hiPSC-F2-3F1 were differentiated towards eye field commitment as described below. When the cultures reached 70-80% confluence, the growth medium was replaced with differentiation medium [DM: DMEM/F12, 4% knockout serum replacement (KOSR), 4% fetal bovine serum (FBS), 1× non-essential amino acids (NEAA), 1× Glutamax, 1× Pen-Strep; Thermo Fisher Scientific] to induce spontaneous differentiation for 2 days. Subsequently, the cultures were shifted to retinal differentiation medium (RDM: DM plus 2% B27) and maintained for 1 month to induce eye field specification. Noggin was omitted from the RDM cocktail in order that uninhibited TGFβ and BMP intrinsic signals could direct OSE development. The distinct EFP clusters that emerged at 4 weeks were either continued as adherent cultures *in situ* or excised manually for suspension cultures as described below.

Corneal differentiation of eye field clusters

The EFPs were further continued *in situ* as adherent cultures in RDM for another 4 weeks to allow whole eyeball-like structure development, with transparent CP on the surface and NR cup on the basal side. These cultures were maintained in corneal differentiation medium (CDM: DM plus 1% N2, 5 µg/ml insulin, 5 ng/ml FGF, 10 ng/ml EGF; Thermo Fisher Scientific) for a further 6-8 weeks to enable maturation of the ocular surface structures. However, a majority of the EFPs gave rise to concentric cell outgrowths, as described previously (Hayashi et al., 2016). Alternatively, the EFPs were manually scooped out intact and cultured in RDM for 4 weeks in non-adherent plates. It is crucial to excise the EFPs at 4 weeks before the commencement of initial waves of surface ectodermal cell and NCC migration. Within 2 weeks of suspension culture, distinct RP and transparent, bubble-like CP structures emerged from the floating EFPs. At 6-8 weeks of differentiation, the delicate CP structures were dissected out of floating EFPs and cultured separately for a further 8-10 weeks in CDM for tissue maturation, as depicted in Fig. 1A. Alternatively, the MCs were processed directly for explant cultures or RNA isolation or fixed in 10% formalin for IHC examination.

Explant culture of MCs

MCs at different stages of maturation (6-10 weeks) were taken and the basal stalk that carries the niche-like organizer along with the adjoining epithelium was chopped out under a microscope and cut into fine pieces in a few drops of CDM. The tissue explants were picked using a needle and explanted on to the surface of de-epithelialized human amniotic membrane (hAM). Alternatively, the explants were placed on Matrigel-coated glass coverslips. The cultures were maintained in CDM and incubated at 37°C with 5% CO_2. The epithelial cells migrated out of the explants and formed growth zones that merged with each other to form uniform epithelial sheets within 10 days. The cell sheets were fixed and processed for IHC examination as described below.

Genomic PCR and semi-quantitative reverse-transcription PCR

Genomic DNA and total RNA were isolated from cell samples using standard procedures. cDNAs were prepared by reverse transcription using the SuperScript II reverse transcriptase kit (Invitrogen, Life Technologies). PCRs were performed using either genomic DNA or cDNA as the reaction template (n=3). Template concentrations were normalized based on *eEF1α* (*EEF1A1*) expression. Table S1 summarizes the primers used. The amplicons were resolved on 1% (w/v) agarose gels, stained with ethidium bromide and imaged using the Gel Doc XR+ system (Bio-Rad).

Immunohistochemistry and image analysis

The MCs were fixed in 10% formalin and paraffin embedded for further sectioning. Thin (4 µm) sections were processed for evaluation by H&E, PAS and Alcian Blue staining by standard procedures. For IHC examination, antigen retrieval was achieved by heating at 100°C with sodium citrate buffer (pH 6.2) and the slides were processed for blocking and antibody incubations. DAB staining of samples was performed as per the manufacturer's instructions (Super Sensitive One-Step Polymer-HRP

Development (2017) 144, 2338-2351 doi:10.1242/dev.143040

IHC detection system, Biogenex), with counterstaining with Hematoxylin, propidium iodide (PI) or DAPI (1 µg/ml each). Table S2 summarizes the antibodies used, including dilutions. Alkaline phosphatase staining was undertaken as per manufacturer's instruction (Chemicon, Millipore). The samples were finally mounted with DPX (SD Fine Chemicals) or glycerol and imaged using an epifluorescence (IX71, Olympus) or confocal (LSM 510, Carl Zeiss) microscope. The images were analyzed using ImagePro Express (Media Cybernetics) and LSM 510 Meta version 3.2 (Carl Zeiss) software, respectively, and the composites were prepared using Adobe Photoshop CS.

Teratoma formation assay

iPSCs at passage 25 were suspended in 20% Matrigel in DMEM/F12 and kept on ice. About 1×10^6 cells in 200 µl were aspirated into tuberculin syringes fitted with a 26 G needle and injected into the subcutaneous space above the rear right haunch of 6-week-old nude mice (n=8). Teratomas that developed at 6-8 weeks post-injection were surgically dissected after euthanizing the animals. The tissues were fixed overnight in 4% paraformaldehyde and processed for paraffin embedding. The tissue blocks were sectioned and processed for IHC examination as described above.

Karyotyping assay

The cells at passage 8 and 20 were grown under standard iPSC culture conditions. About 70-80% confluent cultures were treated with colcemid (0.1 µg/ml; Sigma-Aldrich) for 2-3 h to induce metaphase arrest and trypsinized to prepare single-cell suspensions. The cells were further treated with a hypotonic solution, fixed and then dropped onto clean glass slides (Fisher Scientific) and air dried. After a brief trypsin treatment, the chromosomes were G-banded by Giemsa staining. Well-spread metaphases were imaged and analyzed using CytoVision automated (Applied Imaging).

Transmission electron microscopy (TEM)

Tissues were fixed in 2.5% glutaraldehyde in 0.1 M phosphate buffer (pH 7.2) for 24 h at 4°C and then washed with 1× PBS thoroughly and post-fixed in 1% aqueous osmium tetroxide for 2 h. The samples were then washed, dehydrated through a graded alcohol series, embedded in Spurr's resin and incubated at 80°C for 72 h for complete polymerization. Ultra thin (60 nm) sections were prepared using an ultramicrotome (Leica Ultra Cut UCT-GA-D/E-1/00), mounted on copper grids and stained with saturated aqueous uranyl acetate and counterstained with Reynolds lead citrate. The sections were viewed using a Hitachi H-7500.

Statistics

The mean values of experimental repeats are given as ±s.d.

Acknowledgements

We thank Dr M. Lakshman of the RUSKA Lab, College of Veterinary Sciences, Prof. Jayshankar Telangana State Agricultural University (PJTSAU), Rajendranagar, Hyderabad, India, for providing TEM support; Dr Lakshmi Rao Kandukuri, Clinical Research Facility-Medical Biotechnology (CRF-MB), Centre for Cellular and Molecular Biology (CCMB), Hyderabad, India, for karyotyping; Dr Suresh Pothani, National Centre for Laboratory Animal Sciences, National Institute of Nutrition, Hyderabad, India, for providing animal facility support; and Prof. Dorairajan Balasubramanian, Dr S. Shivaji and Dr Gullapalli Nageshwara Rao for their critical review and useful suggestions in finalizing the manuscript.

Competing interests

The authors declare no competing or financial interests.

Author contributions

Conceptualization: P.J.S., S.M., I.M.; Methodology: P.J.S., S.M., V.K.P., S.R.B., R.R.N., M.N.N., G.B.R., I.M.; Software: I.M.; Validation: P.J.S., S.M., V.K.P., S.R.B., R.R.N., I.M.; Formal analysis: P.J.S., S.M., V.K.P., S.R.B., M.N.N., G.B.R., I.M.; Investigation: P.J.S., S.M., V.K.P., S.R.B., R.R.N., G.B.R., I.M.; Resources: V.K.P., S.R.B., R.R.N., M.N.N., G.B.R., V.S.S., I.M.; Data curation: P.J.S., V.K.P., I.M.; Writing - original draft: P.J.S., I.M.; Writing - review & editing: P.J.S., S.M., V.K.P., S.R.B., V.S.S., I.M.; Visualization: P.J.S., S.M., V.K.P., S.R.B., I.M.; Supervision: S.M., R.R.N., G.B.R., V.S.S., I.M.; Project administration: G.B.R., V.S.S., I.M.; Funding acquisition: V.S.S., I.M.

Funding

This study was supported by grants to I.M. and V.S.S. from the Department of Biotechnology, Ministry of Science and Technology, Government of India (BT/01/COE/06/02/10); Champalimaud Foundation; Tej Kohli Foundation; and the Hyderabad Eye Research Foundation.

Supplementary information

Supplementary information available online at
http://dev.biologists.org/lookup/doi/10.1242/dev.143040.supplemental

References

Ahmad, S., Stewart, R., Yung, S., Kolli, S., Armstrong, L., Stojkovic, M., Figueiredo, F. and Lako, M. (2007). Differentiation of human embryonic stem cells into corneal epithelial-like cells by in vitro replication of the corneal epithelial stem cell niche. *Stem Cells* **25**, 1145-1155.

Assawachananont, J., Mandai, M., Okamoto, S., Yamada, C., Eiraku, M., Yonemura, S., Sasai, Y. and Takahashi, M. (2014). Transplantation of embryonic and induced pluripotent stem cell-derived 3D retinal sheets into retinal degenerative mice. *Stem Cell Rep.* **2**, 662-674.

Basu, S., Sureka, S. P., Shanbhag, S. S., Kethiri, A. R., Singh, V. and Sangwan, V. S. (2016). Simple limbal epithelial transplantation: long-term clinical outcomes in 125 cases of unilateral chronic ocular surface burns. *Ophthalmology* **123**, 1000-1010.

Baulmann, D. C., Ohlmann, A., Flügel-Koch, C., Goswami, S., Cvekl, A. and Tamm, E. R. (2002). Pax6 heterozygous eyes show defects in chamber angle differentiation that are associated with a wide spectrum of other anterior eye segment abnormalities. *Mech. Dev.* **118**, 3-17.

Chan, A. A., Hertsenberg, A. J., Funderburgh, M. L., Mann, M. M., Du, Y., Davoli, K. A., Mich-Basso, J. D., Yang, L. and Funderburgh, J. L. (2013). Differentiation of human embryonic stem cells into cells with corneal keratocyte phenotype. *PLoS ONE* **8**, e56831.

Chen, P., Chen, J. Z., Shao, C. Y., Li, C. Y., Zhang, Y. D., Lu, W. J., Fu, Y., Gu, P. and Fan, X. (2015). Treatment with retinoic acid and lens epithelial cell-conditioned medium in vitro directed the differentiation of pluripotent stem cells towards corneal endothelial cell-like cells. *Exp. Ther. Med.* **29**, 351-360.

Cotsarelis, G., Cheng, S.-Z., Dong, G., Sun, T.-T. and Lavker, R. M. (1989). Existence of slow-cycling limbal epithelial basal cells that can be preferentially stimulated to proliferate: implications on epithelial stem cells. *Cell* **57**, 201-209.

Eiraku, M., Takata, N., Ishibashi, H., Kawada, M., Sakakura, E., Okuda, S., Sekiguchi, K., Adachi, T. and Sasai, Y. (2011). Self-organizing optic-cup morphogenesis in three-dimensional culture. *Nature* **472**, 51-56.

Findlater, G. S., McDougall, R. D. and Kaufman, M. H. (1993). Eyelid development, fusion and subsequent reopening in the mouse. *J. Anat.* **183**, 121-129.

Foster, J. W., Wahlin, K., Adams, S. M., Birk, D. E., Zack, D. J. and Chakravarti, S. (2017). Cornea organoids from human induced pluripotent stem cells. *Sci. Rep.* **7**, 41286.

Gonzalez-Cordero, A., West, E. L., Pearson, R. A., Duran, Y., Carvalho, L. S., Chu, C. J., Naeem, A., Blackford, S. J. I., Georgiadis, A., Lakowski, J. et al. (2013). Photoreceptor precursors derived from three-dimensional embryonic stem cell cultures integrate and mature within adult degenerate retina. *Nat. Biotechnol.* **31**, 741-747.

Grocott, T., Johnson, S., Bailey, A. P. and Streit, A. (2011). Neural crest cells organize the eye via TGF-β and canonical Wnt signalling. *Nat. Commun.* **2**, 265.

Hayashi, R., Ishikawa, Y., Ito, M., Kageyama, T., Takashiba, K., Fujioka, T., Tsujikawa, M., Miyoshi, H., Yamato, M., Nakamura, Y. et al. (2012). Generation of corneal epithelial cells from induced pluripotent stem cells derived from human dermal fibroblast and corneal limbal epithelium. *PLoS ONE* **7**, e45435.

Hayashi, R., Ishikawa, Y., Sasamoto, Y., Katori, R., Nomura, N., Ichikawa, T., Araki, S., Soma, T., Kawasaki, S., Sekiguchi, K. et al. (2016). Co-ordinated ocular development from human iPS cells and recovery of corneal function. *Nature* **531**, 376-380.

Hiler, D., Chen, X., Hazen, J., Kupriyanov, S., Carroll, P. A., Qu, C., Xu, B., Johnson, D., Griffiths, L., Frase, S. et al. (2015). Quantification of retinogenesis in 3D cultures reveals epigenetic memory and higher efficiency in ipscs derived from rod photoreceptors. *Cell Stem Cell* **17**, 101-115.

Huang, J., Dattilo, L. K., Rajagopal, R., Liu, Y., Kaartinen, V., Mishina, Y., Deng, C.-X., Umans, L., Zwijsen, A., Roberts, A. B. et al. (2009). FGF-regulated BMP signaling is required for eyelid closure and to specify conjunctival epithelial cell fate. *Development* **136**, 1741-1750.

Inamdar, M. S., Venu, P., Srinivas, M. S., Rao, K. and VijayRaghavan, K. (2009). Derivation and characterization of two sibling human embryonic stem cell lines from discarded grade III embryos. *Stem Cells Dev.* **18**, 423-434.

Kaewkhaw, R., Kaya, K. D., Brooks, M., Homma, K., Zou, J., Chaitankar, V., Rao, M. and Swaroop, A. (2015). Transcriptome dynamics of developing photoreceptors in three-dimensional retina cultures recapitulates temporal sequence of human cone and rod differentiation revealing cell surface markers and gene networks. *Stem Cells* **33**, 3504-3518.

Kanakubo, S., Nomura, T., Yamamura, K.-I., Miyazaki, J.-I., Tamai, M. and Osumi, N. (2006). Abnormal migration and distribution of neural crest cells in Pax6 heterozygous mutant eye, a model for human eye diseases. *Genes Cells* **11**, 919-933.

Kinoshita, H., Suzuma, K., Kaneko, J., Mandai, M., Kitaoka, T. and Takahashi, M. (2016). Induction of functional 3D ciliary epithelium-like structure from mouse induced pluripotent stem cells. *Invest. Ophthalmol. Vis. Sci.* **57**, 153-161.

Kuwahara, A., Ozone, C., Nakano, T., Saito, K., Eiraku, M. and Sasai, Y. (2015). Generation of a ciliary margin-like stem cell niche from self-organizing human retinal tissue. *Nat. Commun.* **6**, 6286.

Mariappan, I., Kacham, S., Purushotham, J., Maddileti, S., Siamwala, J. and Sangwan, V. S. (2014). Spatial distribution of niche and stem cells in ex vivo human limbal cultures. *Stem Cells Transl. Med.* **3**, 1331-1341.

Mariappan, I., Maddileti, S., Joseph, P., Siamwala, J. H. and Vauhini, V. (2015). Enriched cultures of retinal cells from BJNhem20 human embryonic stem cell line of Indian origin. *Invest. Ophthalmol. Vis. Sci.* **56**, 6714-6723.

Marko, C. K., Tisdale, A. S., Spurr-Michaud, S., Evans, C. and Gipson, I. K. (2014). The ocular surface phenotype of Muc5ac and Muc5b null mice. *Invest. Ophthalmol. Vis. Sci.* **55**, 291-300.

McCabe, K. L., Kunzevitzky, N. J., Chiswell, B. P., Xia, X., Goldberg, J. L. and Lanza, R. (2015). Efficient generation of human embryonic stem cell-derived corneal endothelial cells by directed differentiation. *PLoS ONE* **10**, e0145266.

McKenzie, R. W., Jumblatt, J. E. and Jumblatt, M. M. (2000). Quantification of MUC2 and MUC5AC transcripts in human conjunctiva. *Invest. Ophthalmol. Vis. Sci.* **41**, 703-708.

Mikhailova, A., Ilmarinen, T., Uusitalo, H. and Skottman, H. (2014). Small-molecule induction promotes corneal epithelial cell differentiation from human induced pluripotent stem cells. *Stem Cell Rep.* **2**, 219-231.

Rama, P., Matuska, S., Paganoni, G., Spinelli, A., De Luca, M. and Pellegrini, G. (2010). Limbal stem-cell therapy and long-term corneal regeneration. *N. Engl. J. Med.* **363**, 147-155.

Ramirez-Miranda, A., Nakatsu, M. N., Zarei-Ghanavati, S., Nguyen, C. V. and Deng, S. X. (2011). Keratin 13 is a more specific marker of conjunctival epithelium than keratin 19. *Mol. Vis.* **17**, 1652-1661.

Reichman, S., Terray, A., Slembrouck, A., Nanteau, C., Orieux, G., Habeler, W., Nandrot, E. F., Sahel, J.-A., Monville, C. and Goureau, O. (2014). From confluent human iPS cells to self-forming neural retina and retinal pigmented epithelium. *Proc. Natl. Acad. Sci. USA* **111**, 8518-8523.

Richardson, R. J., Hammond, N. L., Coulombe, P. A., Saloranta, C., Nousiainen, H. O., Salonen, R., Berry, A., Hanley, N., Headon, D., Karikoski, R. et al. (2014). Periderm prevents pathological epithelial adhesions during embryogenesis. *J. Clin. Invest.* **124**, 3891-3900.

Sangwan, V. S., Basu, S., Vemuganti, G. K., Sejpal, K., Subramaniam, S. V., Bandyopadhyay, S., Krishnaiah, S., Gaddipati, S., Tiwari, S. and Balasubramanian, D. (2011). Clinical outcomes of xeno-free autologous cultivated limbal epithelial transplantation: a 10-year study. *Br. J. Ophthalmol.* **95**, 1525-1529.

Sareen, D., Saghizadeh, M., Ornelas, L., Winkler, M. A., Narwani, K., Sahabian, A., Funari, V. A., Tang, J., Spurka, L., Punj, V. et al. (2014). Differentiation of human limbal-derived induced pluripotent stem cells into limbal-like epithelium. *Stem Cells Transl. Med.* **3**, 1002-1012.

Schermer, A., Galvin, S. and Sun, T. T. (1986). Differentiation-related expression of a major 64K corneal keratin in vivo and in culture suggests limbal location of corneal epithelial stem cells. *J. Cell Biol.* **103**, 49-62.

Shalom-Feuerstein, R., Serror, L., De La Forest Divonne, S., Petit, I., Aberdam, E., Camargo, L., Damour, O., Vigouroux, C., Solomon, A., Gaggioli, C. et al. (2012). Pluripotent stem cell model reveals essential roles for miR-450b-5p and miR-184 in embryonic corneal lineage specification. *Stem Cells* **30**, 898-909.

Sidney, L. E., Branch, M. J., Dunphy, S. E., Dua, H. S. and Hopkinson, A. (2014). Concise review: evidence for CD34 as a common marker for diverse progenitors. *Stem Cells* **32**, 1380-1389.

Takahashi, K., Tanabe, K., Ohnuki, M., Narita, M., Ichisaka, T., Tomoda, K. and Yamanaka, S. (2007). Induction of pluripotent stem cells from adult human fibroblasts by defined factors. *Cell* **131**, 861-872.

Völkner, M., Zschätzsch, M., Rostovskaya, M., Overall, R. W., Busskamp, V., Anastassiadis, K. and Karl, M. O. (2016). Retinal organoids from pluripotent stem cells efficiently recapitulate retinogenesis. *Stem Cell Rep.* **6**, 525-538.

Yoshida, S., Shimmura, S., Kawakita, T., Miyashita, H., Den, S., Shimazaki, J. and Tsubota, K. (2006). Cytokeratin 15 can be used to identify the limbal phenotype in normal and diseased ocular surfaces. *Invest. Ophthalmol. Vis. Sci.* **47**, 4780-4786.

Zhang, K., Pang, K. and Wu, X. (2014). Isolation and transplantation of corneal endothelial cell-like cells derived from *in-vitro*-differentiated human embryonic stem cells. *Stem Cells Dev.* **23**, 1340-1354.

Zhong, X., Gutierrez, C., Xue, T., Hampton, C., Vergara, M. N., Cao, L.-H., Peters, A., Park, T. S., Zambidis, E. T., Meyer, J. S. et al. (2014). Generation of three-dimensional retinal tissue with functional photoreceptors from human iPSCs. *Nat. Commun.* **5**, 4047.